

# Robust Lung Ventilation Assessment

Sven Kabus<sup>1</sup>, Tobias Klinder<sup>1</sup>, Tokihiro Yamamoto<sup>2</sup>,  
Paul J. Keall<sup>3</sup>, Billy W. Loo, Jr.<sup>4</sup>, and Cristian Lorenz<sup>1</sup>

<sup>1</sup> Philips Research Laboratories, Hamburg, Germany  
sven.kabus@philips.com

<sup>2</sup> Dep. of Radiation Oncology, University of California Davis, Sacramento, USA

<sup>3</sup> Sydney Medical School, University of Sydney, Sydney, Australia

<sup>4</sup> Dep. of Radiation Oncology, Stanford University School of Medicine, Stanford, USA

**Abstract.** Estimation of local lung ventilation from dynamic CT acquisition becomes an interesting alternative to nuclear imaging as it offers several advantages such as higher spatial resolution or comparably low cost. Current approaches evaluate the ventilation as voxel-wise volume change separately for each phase and thus neglect the dynamic aspects of the respiratory system which leads to a less robust estimation. In this paper, we propose a novel ventilation assessment that considers the voxel-wise volume change over the entire breathing cycle by incorporating a prior model. We show that our new method results in more plausible estimates of the local volume change. It also yields the quantification of phase shifts within the lungs that may have additional clinical utility. Moreover, we are able to automatically detect image regions with non-plausible volume changes potentially caused by image artifacts.

## 1 Introduction

Ventilation is the primary function of the respiratory system. In particular, assessing ventilation on a local or regional level becomes increasingly important for diagnosis, e.g., for early detection of diseases [1], or for therapy planning, e.g., for functional avoidance in lung cancer radiotherapy [2].

Nuclear imaging such as SPECT or PET are the current standard for direct functional assessment of lung ventilation, but suffer from low spatial resolution, high cost, long scan time and/or low accessibility.

In order to overcome the limitations, the use of respiratory phase-based gated 4D CT (3D+t) has been proposed. The basic idea is to first estimate deformation fields from one selected reference to all other phases which can then be analyzed to obtain the voxel-wise volume change over the respiratory cycle [3–5].

The estimation of local volume changes is affected by multiple sources of error, such as, e.g., imaging artifacts, binning artifacts or image noise. Especially imaging or binning artifacts, which can be spread over many slices, lead to non-optimal input data for the registration and may significantly infer the local volume change estimation. Examples of such artifacts include duplicate diaphragm contours or missing structures in one or both data sets to be registered. Unfortunately, imaging or binning artifacts are very common in dynamic

acquisitions as diseased patients have problems in breathing reproducibly: It was found that for 90% of 4D CT acquisitions artifacts of 4mm and more occur in at least one respiratory phase [6].

So far, most approaches typically compute the local volume change individually between two phases and do not consider all phases simultaneously [3–5]. Taking the dynamic aspects into account, i.e. looking at the voxel-wise volume change over the whole breathing cycle, is however crucial as this allows to increase the robustness against different sources of errors. In the context of deformation field estimation, few approaches have recently considered the dynamical behavior of the displacement per voxel by performing a trajectory constrained 4D registration [7, 8]. Instead of performing separate phase-to-phase registration, all phases are considered simultaneously which, however, results in a higher computational effort.

Here, we propose a novel concept, making use of the entire dynamic information for a robust estimation of local volume change over the whole breathing cycle. A functional model is applied regionally and fitted to the local volume change. This results in more plausible estimates of voxel-wise volume change. In addition, the deviation from the model can be used as an indicator for image locations with non-plausible volume changes that are potentially caused by image artifacts.

## 2 Method

### 2.1 Image Data

We used 4D CT scans of 12 patients that were acquired for radiotherapy treatment. During the CT scan, patient respiratory traces were acquired using the Varian RPM system (Varian Medical Systems, Palo Alto, CA), with the marker block placed on the upper abdomen. Acquisition was done in cine mode. The projection images were retrospectively sorted into ten respiratory phase-based bins of 3D CT image data (i.e., from 0% to 90% phase at 10% intervals, where 0% typically corresponds to end-inhale and 60% to end-exhale). The end-inhale phase and the end-exhale phase were carefully selected by a radiologist. All images had an in-plane resolution of 0.85-0.97mm and a slice thickness of 2.5mm.

### 2.2 Robust Functional Lung Analysis

Our proposed method consists of three main building blocks. First, deformation fields are calculated to establish a voxel-wise correspondence between all phases of the 4D CT. The deformation fields are then analyzed yielding a first estimate of the local volume change. In contrast to former work, we do not treat the local volume change per phase separately, but extend the estimation by fitting a prior model to the relative volume change of each voxel to obtain a robust and compact dynamic representation. Each building block is explained in detail in the following.

**Computation of deformation vector field.** In a registration step, the deformation vector fields (DVF) between a selected reference, usually the 0% phase, and all other respiratory phases are determined. For the computation of the DVFs, we use a fully-automatic volumetric elastic registration scheme [9] that maps the reference phase onto all other phases and thus establishes a voxel-wise correspondence over the whole breathing cycle. The registration scheme requires either a lung mask or a pre-processing of the input images in order to avoid mis-alignment of near-pleura parenchymal structures due to potential sliding along the lung-rib interface. Here, a pre-processing in terms of a simple transfer function is applied to the image intensity scale. By choosing a smooth transfer function, such that intensities smaller than 0HU are preserved and intensities larger than 0HU are mapped to 0HU, bone structures become of similar intensity than surrounding tissue and, therefore, rib cage motion does not influence lung motion. As common for many state-of-the-art registration schemes, a joint functional consisting of a similarity measure and a regularizer is minimized. For the similarity measure, sum of squared differences is chosen while the regularizer is defined as a linear elastic model. Based on calculus of variations a system of non-linear partial differential equations is to be solved. The iterative solution is stopped if either the update in the deformation is below 0.05mm for all voxel positions (indicating convergence) or the Jacobian of the deformation is below 0.1 (guaranteeing the absence of singularities). The registration accuracy has shown to be in the subvoxel range [9].

**Computation of ventilation trajectory.** In contrast to former work, we extend the estimation of the local volume change by considering also the temporal behavior. For that purpose, from each DVF  $u^{0\% \rightarrow i\%}$ ,  $i = 10, 20, \dots, 90$ , the voxel-wise volume change is derived by calculating the Jacobian  $V^{0\% \rightarrow i\%}(x) := \det(\nabla u^{0\% \rightarrow i\%}(x))$  for each voxel  $x$  of the DVF. The Jacobian estimates how much the region around this voxel is contracting or expanding. A value of 1 corresponds to volume preservation whereas a value smaller (larger) than 1 indicates local compression (expansion). For each voxel  $x$ , a vector is constructed as  $V(x) := (1, V^{0\% \rightarrow 10\%}(x), V^{0\% \rightarrow 20\%}(x), \dots, V^{0\% \rightarrow 90\%}(x))$  describing the volume change over the breathing cycle, the so-called ventilation trajectory as a trajectory in the temporal domain (see Fig. 1 for examples).

**Model fit to ventilation trajectory.** In order to arrive at a more robust and compact representation of the volume change over the breathing cycle, we perform a model fit to the ventilation trajectory  $V$ . The 1D model is based on a  $\cos^{2n}$  function as it is frequently used (see, e.g., [10, 11]) to describe the lung volume  $\text{vol}(t)$  over the respiratory cycle. Inspired by this representation, we apply the same function to the relative volume change that we consider here. The relative volume change with respect to a designated reference phase (here 0% phase) is given as  $\text{vol}(t)/\text{vol}(t_{0\%})$ . By subtracting 1, we have

$$\frac{\text{vol}(t)}{\text{vol}(t_{0\%})} - 1 = \frac{\text{vol}(t) - \text{vol}(t_{0\%})}{\text{vol}(t_{0\%})} =: \frac{\Delta \text{vol}(t)}{\text{vol}(t_{0\%})}$$

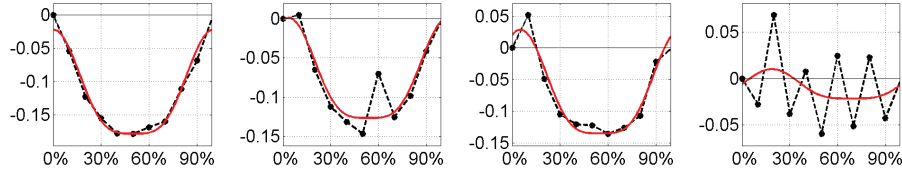


**Fig. 1.** Examples for ventilation trajectory  $V$  (shown in black) and fitted model  $V^{model}$  (red) for different lung positions. The first example (from left) shows a trivial fit whereas the second example demonstrates an outlier causing the amplitude to be underestimated for the standard approach but not for the proposed method. The third example shows a slight phase shift, inhalation is not deepest for the 0% phase. For the last example a fit is not plausible which can be detected by a large fit error  $E$ .

which is widely used in the definition of lung ventilation (see, e.g. [5]). Assuming that  $\text{vol}(t)$  can be described by a  $\cos^{2n}$ -based function, the model should thus also hold for the relative volume change.

With  $l = 10$  denoting the number of respiratory phases,  $o$  an offset,  $\alpha$  representing the ventilation amplitude and  $\phi$  the time of end-exhalation, the function

$$V^{model}(x, t) = o + \alpha \cos^{2n} \left( \frac{\pi}{l}(t - \phi) + \frac{\pi}{2} \right)$$

describes the ventilation at time  $t$  for a fixed anatomical position  $x$ . The model parameter  $n$  is chosen to place emphasis on the exhalation state which is usually longer than the inhalation state (typically,  $n = 2$ ). The ventilation model  $V^{model}$  is fitted to the ventilation trajectory  $V$  by a least-squares optimization, here implemented by a Gauß-Newton scheme. A few actual examples of ventilation trajectories together with their fitted model functions are shown in Fig. 1.

Another interesting parameter that can be calculated using the model representation is the squared difference between fitted model and trajectory weighted with the inverse of the ventilation amplitude, the so-called fit error

$$E(x) := \frac{1}{\max(\alpha(x), \epsilon)} \|V^{model}(x, t) - V(t)\|_2.$$

It is used in the following as a confidence level for the ventilation estimate.

### 2.3 Error Detection

The error term  $E$  measures the deviation of the ventilation from the model. Assuming that the model is an adequate representation, an accurate ventilation should result in a small error. Consequently, a local large error  $E$  should reveal areas of misregistration or of inaccurate ventilation estimation caused by imperfect image data, e.g., due to breathing artifacts. While having such region identified is a benefit in itself, we can also go one step further and perform a *second* registration in those critical areas with different registration settings which will then result in more plausible local ventilation.

In order to test the value of the error term, we generated synthetic images on which error detection was carried out. Finally, a second-pass registration scheme was used aiming at an improved ventilation estimate.

**Synthetic Data.** To evaluate the performance of the second-pass registration, ground-truth is required. Careful selection of data sets was done to find cases that were less impacted by breathing or binning artifacts. For two of such cases a slab of eight slices located in the lower lungs was modified in three different ways: (A) cyclic shift by one respiratory phase, (B) reduced exhalation depth, (C) reduced inhalation depth. Setting A replaced the slab with data from the preceding respiratory phase. Setting B (C) doubled the end-inhalation (end-exhalation) phases and skipped the end-exhalation (end-inhalation) phases within the slab. These synthetic modifications mimic the type of error frequently found in real image data.

**Second pass registration.** Image regions with a larger fit error are likely to be impacted by image artifacts. To exclude those regions from driving the registration process, a weighting mask is added to the registration scheme. The basic idea is to upweight the regularizer here, thus to assign a low weight to image voxels with a large fit error  $E$ . Therefore, from  $E$  two thresholds  $t^{lower}$ ,  $t^{upper}$  are generated (here we took the 80% and the 95% quantiles). A weight of 0 (1) is assigned to voxels with a fit error  $E(x)$  larger (smaller) than the upper (lower) threshold. For the remaining voxels a linear mapping is chosen,

$$M(x) = \begin{cases} 0 & : E(x) > t^{upper} \\ \frac{t^{upper} - E(x)}{t^{upper} - t^{lower}} & : t^{lower} < E(x) < t^{upper} \\ 1 & : E(x) < t^{lower} \end{cases} .$$

The building blocks as described in Sect. 2.2 are now executed again – in contrast to the first-pass registration now with the weighting mask  $M$  as additional factor within the similarity measure.

### 3 Results

The benefit for the novel robust lung ventilation is demonstrated in two different experiments. First, we compare the method to the state of the art for lung ventilation in Sect. 3.1. At second, we show the value of evaluating the error term for identifying regions corrupted by image artifacts.

#### 3.1 Robust Lung Ventilation

Evaluating the accuracy of the estimated voxel-wise local ventilation is extremely difficult due to a lack of ground truth. Comparing, e.g., the 4D CT-based ventilation estimation with that obtained from nuclear imaging [3] suffers from low resolution and artifacts in the nuclear images. Also, determining the accuracy of the underlying deformation fields is not sufficient since ventilation estimation can differ significantly even for methods showing similar target registration errors [12].

However, even without an established ground truth, we are still able to compare two different ventilation estimates as we expect certain characteristics from the estimation given the fact that it reflects a physiological process: for example, with the lung at end-inhale as the reference position, an overall contraction – rather than a mixture of contracting and expanding regions – seems to be desirable from a physiological point of view. In addition, the radiologist’s selection of end-inhale and end-exhale phase does not necessarily hold for the entire lungs. A suboptimal choice will result in under-estimating the ventilation amplitude, thus increases its inhomogeneity. As a measure for inhomogeneity, the variance of the assessed ventilation amplitude was computed. Evaluation on 12 data sets resulted in a variance of 0.004 to 0.016 and of 0.002 to 0.010 using end-inhale/end-exhale phases and all phases, respectively (see Tab. 1). In all cases, the variance was reduced for the proposed method, mean improvement was computed as 38%.

case ID	inhale/exhale		all phases used	
	mean	variance	mean	variance
01	0.244	0.012	0.242	0.008
02	0.087	0.004	0.098	0.002
03	0.268	0.016	0.241	0.010
04	0.087	0.004	0.092	0.002
05	0.203	0.012	0.197	0.008
06	0.052	0.004	0.066	0.002
07	0.158	0.007	0.166	0.003
08	0.107	0.004	0.107	0.002
09	0.223	0.008	0.220	0.006
10	0.160	0.004	0.167	0.004
11	0.188	0.006	0.179	0.004
12	0.161	0.012	0.162	0.008

**Table 1.** Mean and variance of assessed ventilation amplitude based on (i) only the end-inhale and end-exhale image pair and (ii) all respiration phases.

Fig. 2 compares the ventilation estimate based on end-inhale and end-exhale phase (marked in blue) with the ventilation estimate based on all phases (bottom). Overall, the proposed method results in a more homogeneous map. Focusing on the upper left lobe a mixed pattern of contraction and expansion can be observed for any  $V^{0\% \rightarrow i\%}$ . Careful inspection revealed a phase shift (see Fig. 1(c) for an example) causing this unrealistic pattern – the 0% phase and the 60% phase do not contain the extremal states for this lung region. The proposed method, however, provides a realistic amplitude by shifting the trajectory along the respiratory cycle.

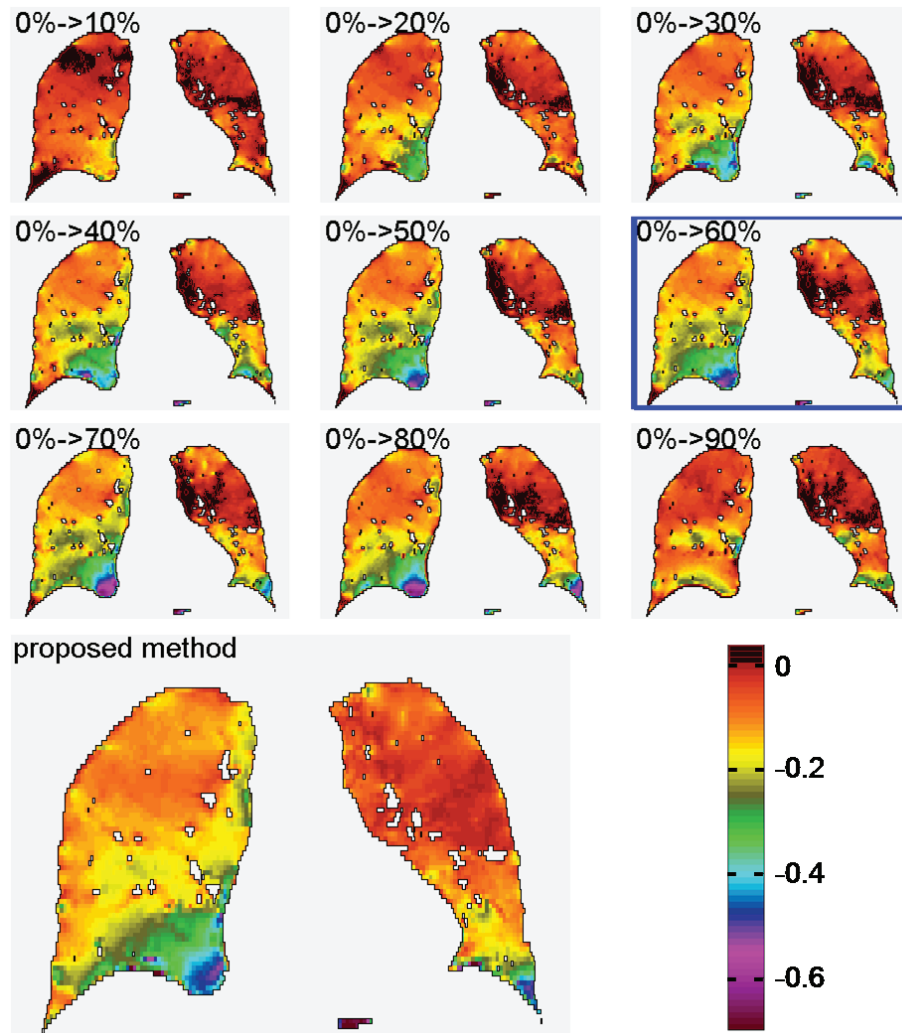


**Fig. 2.** Volume change over the respiratory cycle (top 3x3) and ventilation amplitude  $\alpha$  (bottom) after fitting to the ventilation model. The result from a state-of-the-art approach (see text) is marked blue. Note the inhomogeneous pattern in the upper left lobe with regions showing even positive values.

### 3.2 Error Detection

Slab modifications as described in Sect. 2.3 for the settings A-C affect ventilation assessment. Fig. 3 (left) shows that a reduced inhalation depth (setting C) results in a reduced amplitude in lung regions above the modified slab, a reduced exhalation depth (setting B) decreases the amplitude within the slab. Moreover, the cyclic shift (setting A) by 10% of the respiratory cycle is correctly estimated as shown in Fig. 3 (center). For all modifications the fit error is increased around the modified slab (cf. Fig. 3 (right) for an example).

From the fit error a mask function (cf. Sect. 2.3) is computed and used as input for a second-pass registration. From the corrected deformation fields the ventilation trajectory for each voxel position is computed. The model fit then results in a smaller fit error within the modified slab, see Fig. 3 (right). In the same way, a binning artifact on top of the diaphragm (slices 95-100) is excluded from driving the registration resulting in a decreased fit error as well. Further analysis is required to ensure the applicability to real image artifacts.

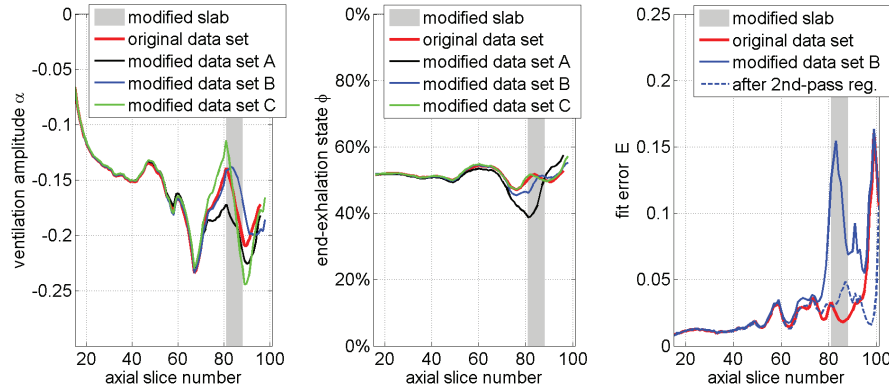


**Fig. 3.** Analysis of slicewise averaged ventilation amplitude (left), end-exhalation state (center) and fit error (right).

## 4 Conclusion

In this paper we show that local lung ventilation can be robustly estimated from 4D CT image data. A physiologically motivated breathing model is applied voxelwise to the volume change curve along the breathing cycle. Volume change is calculated by use of the Jacobian of the deformation vector field. In comparison to ventilation calculation based on only the end-inhale and end-exhale image pair, the presented method is able to take the whole breathing cycle into account for ventilation amplitude calculation. Regionally varying breathing phase shifts

are recognized and do not deteriorate the estimation result. Applied to twelve 4D CT data sets, it could be shown that by taking the whole breathing cycle into account, the ventilation estimation is less impacted by image noise or other image imperfections.

The deviation from the physiological model, expressed as fit error after model adaptation, can be used to detect regions of low image fidelity. It could be shown that synthetically deteriorated image regions can be detected with the presented method and that potentially a second-pass registration can improve the registration result.

## References

1. de Jong, P., Lindblad, A., Rubin, L., et al.: Progression of lung disease on computed tomography and pulmonary function tests in children and adults with cystic fibrosis. *Thorax* **61** (2006) 80–85
2. Yaremko, B., Guerrero, T., Noyola-Martinez, J., et al.: Reduction of normal lung irradiation in locally advanced non-small-cell lung cancer patients, using ventilation images for functional avoidance. *Int J Radiat Oncol* **68** (2007) 562–571
3. Reinhardt, J., Ding, K., Cao, K., et al.: Registration-based estimates of local lung tissue expansion compared to xenon CT measures of specific ventilation. *Med Image Anal* **12** (2008) 752–763
4. Yamamoto, T., Kabus, S., Klinder, T., et al.: 4D computed tomography pulmonary ventilation images vary with deformable image registration algorithms and metrics. *Med Phys* **38** (3) (2011) 1–11
5. Guerrero, T., Sanders, K., Castillo, E., et al.: Dynamic ventilation imaging from 4D computed tomography. *Phys Med Biol* **51** (4) (2006) 777–791
6. Yamamoto, T., Langner, U., Loo, B., Shen, J., Keall, P.: Retrospective analysis of artifacts in four-dimensional CT images of 50 abdominal and thoracic radiotherapy patients. *Int J Radiat Oncol Biol Phys* **72** (4) (2008) 1250–1258
7. Peyrat, J.M., Delingette, H., Sermesant, M., et al.: Registration of 4D time-series of cardiac images with multichannel diffeomorphic demons. In: MICCAI. Volume 5242. (2008) 972–979
8. Castillo, E., Castillo, R., Martinez, J., et al.: 4D deformable image registration using trajectory modeling. *Phys Med Biol* **55** (2010) 305–327
9. Kabus, S., Lorenz, C.: Fast elastic image registration. In: *Medical Image Analysis For The Clinic - A Grand Challenge*. (2010) 81–89
10. Lujan, A., Larsen, E., Balter, J., et al.: A method for incorporating organ motion due to breathing into 3D dose calculations. *Med Phys* **26** (5) (1999) 715–720
11. George, R., Vedam, S., Chung, T., et al.: The application of the sinusoidal model to lung cancer patient respiratory motion. *Med Phys* **32** (9) (2005) 2850–2861
12. Kabus, S., Klinder, T., Murphy, K., et al.: Evaluation of 4D-CT lung registration. In: MICCAI. Volume 5761. (2009) 747–754